Anomalous In-Plane Electronic Scattering in Charge Ordered $Na_{0.41}CoO_2 \cdot 0.6H_2O$

Guixin Cao,[1,2,3,*,†] Maxim M. Korshunov,[4,5,6] Yuze Gao,[1] Mathieu Le Tacon,[1] David J. Singh,[7] and Chengtian Lin[1,*,‡]

[1]*Max-Planck-Institute for Solid State Research, Heisenbergstrasse 1, Stuttgart D-70569, Germany*
[2]*Department of Physics, Shanghai University, Shanghai 200444, PR China*
[3]*Department of Materials Science and Engineering, University of Tennessee, Knoxville, Tennessee 37996, USA*
[4]*Department of Physics, University of Florida, Gainesville, Florida 32611, USA*
[5]*L. V. Kirensky Institute of Physics, Siberian Branch of Russian Academy of Sciences, 660036 Krasnoyarsk, Russia*
[6]*Siberian Federal University, Svobodny Prospect 79, 660041 Krasnoyarsk, Russia*
[7]*Materials Science and Technology Division, Oak Ridge National Laboratory, Oak Ridge, Tennessee 37831-6056, USA*

(Received 18 September 2011; revised manuscript received 1 December 2011; published 6 June 2012)

We report electronic transport measurements on high quality floating zone grown Na_xCoO_2 and $Na_{0.41}CoO_2 \cdot 0.6H_2O$ single crystals. We find an in-plane electronic scattering minimum near 11 K and a clear charge ordering at approximately 50 K. The electronic and magnetic properties in hydrated and nonhydrated $Na_{0.41}CoO_2$ samples are similar at higher temperature, but evolve in markedly different ways below ~50 K, where a strong ferromagnetic tendency is observed in the hydrated sample. Model calculations show the relationship of this tendency to the structure of the Fermi surface. The results, particularly the clear differences between the hydrated and nonhydrated material show a substantially enhanced ferromagnetic tendency upon hydration. Implications for superconductivity are discussed.

DOI: 10.1103/PhysRevLett.108.236401 PACS numbers: 71.30.+h, 72.80.Ga, 75.20.Hr, 75.30.Gw

The interplay of superconductivity and magnetism is particularly interesting in $Na_xCoO_2 \cdot yH_2O$. Except for $x \sim 0.5$, the material is metallic and in close proximity to magnetism, while at $x \sim 1/3$ and with hydration $y \sim 4/3$ it is a superconductor with $T_c \sim 5$ K [1]. There are indications both from theory and experiment that this superconductivity could be triplet in nature, [2–5] although singlet states were also discussed [6]. $T_c = 5$ K is remarkable for a triplet (cf. Sr_2RuO_4 with $T_c < 2$ K) [7]. The question of the superconducting nature and magnetic behavior are intimately connected. However, while there has been substantial work on the magnetism in nonhydrated material for $x > 0.5$, the magnetic behavior for $x < 0.5$ is apparently different and more subtle, and study of the hydrated compounds has been impeded by sample quality issues.

Besides superconductivity, the observed states include magnetic ordering and charge ordering (CO). Interestingly, while Na_xCoO_2 is a correlated oxide, spectroscopies show renormalizations distinct from those expected near a Mott transition, [8] qualitatively like the Fe-based superconductors [9]. For $Na_xCoO_2 \cdot yH_2O$, the question of the symmetry of the superconducting state is intimately connected to the nature of the magnetic fluctuations. Near $x = 0.5$ nonhydrated Na_xCoO_2 shows CO and antiferromagnetism (AFM) [10]. This appears to be intimately connected with Na ordering. For higher x the material shows Curie-Weiss behavior [11–13], and there is a magnetic ordering at low T [14–16]. This ordering, while AFM between the planes, is ferromagnetic (FM) in plane. The magnetic behavior for $x < 0.5$ is more subtle, with Pauli paramagnetism. For superconductivity, FM spin fluctuations are repulsive in singlet channels (s, d) and attractive for triplet superconductivity (p, f) [17,18]. Therefore, in a near two dimensional (2D) material, nearness to in-plane FM implies triplet superconductivity, while antiferromagnetism can be pairing in either triplet or singlet channels, or not pairing at all, depending on the momentum dependence in relation to the Fermi surface (FS). An interesting possibility is that AFM and FM tendencies compete, yielding suppression of magnetic order in favor of superconductivity, as might be the case in Sr_2RuO_4 [19]. Importantly, while hydrated Na_xCoO_2 is superconducting, the metallic nonhydrated material is not. Furthermore, hydrated phases with lower y than the fully hydrated superconductor can be prepared. These have properties intermediate between the fully hydrated superconductor and nonhydrated material. Understanding the differences between these phases can yield understanding of the superconductivity, especially since the partially hydrated phases, while little studied to date, are more amenable to experimental investigation due to their greater stability.

We report investigation of high quality single crystals of nonhydrated and hydrated $Na_{0.41}CoO_2$. We find that the electronic and magnetic properties in nonhydrated and partly hydrated $Na_{0.41}CoO_2$ samples are similar at higher temperature, but evolve differently for temperatures below ~50 K. This correlates with the different evolution of electronic Raman scattering previously found in superconducting hydrated samples [20]. There is an anomalous in-plane electronic scattering minimum at ~11 K and clear transition at ~50 K over a wide range of applied magnetic fields in $Na_xCoO_2 \cdot yH_2O$. Our magnetic measurements show an increasing FM tendency at low temperature in the hydrated sample, which is associated

with the properties of the FS induced by water intercalation in accord with the first principles calculations. The implication is that the superconductivity of fully hydrated $Na_{0.41}CoO_2$ is likely triplet.

Single crystal $Na_{0.41}CoO_2$ was synthesized by deintercalation from a freshly cleaved high quality floating zone grown γ-$Na_{0.74}CoO_2$ crystal in 6.6 mol Br_2/CH_3CN for 78 hours, as in Ref. [21]. The Na content was determined by energy dispersive x-ray including microanalysis. The $2 \times 1 \times 0.1$ mm sample was divided into two parts. One was stored in an evacuated container as a nonhydrated sample. The other part, with four electrodes attached, was placed in a special humidity instrument with stable 90% humidity and 45 °C temperature to obtain a uniformly hydrated crystal. We thus obtained a hydrated sample with H_2O concentration of 0.6. To avoid water loss [20,22], the $Na_{0.41}CoO_2 \cdot 0.6H_2O$ sample was transferred into a vacuum chamber held at 250 K. We checked and confirmed that water content was unchanged after investigation of the physical properties. The Co valence was determined by using redox titrations. The Co valence for $Na_{0.41}CoO_2$ with $\sim$0.6 H_2O is +3.57, +0.02 less than nonhydrated $Na_{0.41}CoO_2$ (+ 3.59), indicating approximate charge balance between the nonhydrated and hydrated phases. Resistance was measured in a physical property measurement system and susceptibilities with a SQUID magnetometer. We emphasize that our samples were stable when handled as above and that all results presented below were reproducible. The Na concentration was confirmed using an inductively coupled plasma spectrometer chemical analysis after physical measurements for nonhydrated and hydrated $Na_{0.41}CoO_2$ samples.

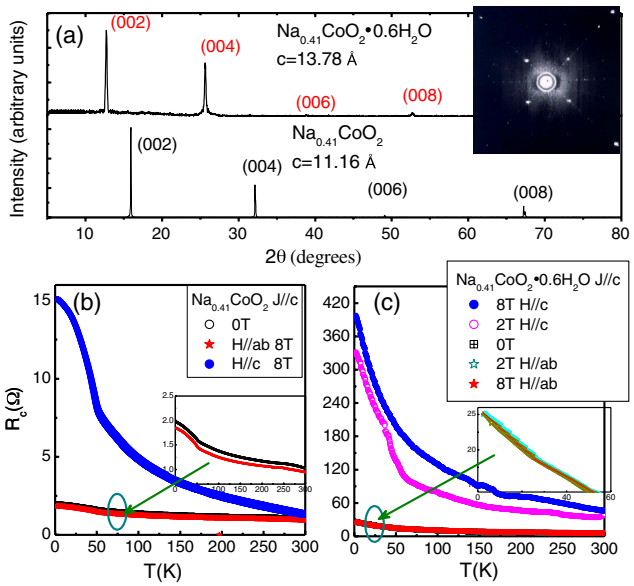

FIG. 1 (color online). (a) XRD patterns of (00l) planes for $Na_{0.41}CoO_2$ and $Na_{0.41}CoO_2 \bullet 0.6H_2O$. Inset shows the Laue patterns after hydration. (b) and (c) give R_c vs T under different H. Inset of (b) and (c) are blowups for $H = 0$ and $H//ab$.

X-ray diffraction (XRD) patterns [Fig. 1(a)] for the hydrated and nonhydrated $Na_{0.41}CoO_2$ show well aligned (00l) planes, indicative of the high sample quality. The reflections shift to the lower 2θ angle direction with hydration. Out-of-plane resistances R_c [Figs. 1(b) and 1(c)], show the larger c-axis resistance of the hydrated $Na_{0.41}CoO_2$ sample. Two established differences for hydrated and nonhydrated systems are (1) the hydrated material is much more two dimensional [15,16,23,24] and (2) there is a remarkably strong interplay between the electronic and magnetic properties of the CoO_2 layers and the Na ordering in the nonhydrated material [25–27]. This is screened upon hydration, reducing the tendency to charge ordering, and revealing novel behavior including superconductivity. However, elucidation of other differences has been impeded by the lack of stable, uniform samples with similar compositions.

Figure 2 gives the in-plane resistivities (ρ_{ab}) as functions of temperature (T) for different magnetic fields (H) with $H \parallel ab$ and $H \parallel c$. The nonhydrated sample [Fig. 2(a)] shows metallic behavior over the whole temperature range. The residual electrical resistivity is $\rho_0 = 21.5\ \mu\Omega$ cm, which is 2 times better than commonly reported [12,28]. For $Na_{0.41}CoO_2 \cdot 0.6H_2O$ [Fig. 2(b)], transitions are seen in resistivity at $\sim$51 K and $\sim$11 K. The 51 K transition is quite similar to that in $Na_{0.5}CoO_2$, where there is a charge ordering transition T_{CO}. It must be noted that a similar CO was observed by Wang *et al.* [29] in a hydrated $Na_{0.41}CoO_2$ compound, made by immersion in distilled water. Field has a remarkable effect on ρ_{ab} of $Na_{0.41}CoO_2 \cdot 0.6H_2O$ especially below 50 K, but a negligible effect on ρ_{ab} of $Na_{0.41}CoO_2$. The inset of Fig. 2(b) gives a schematic repre-

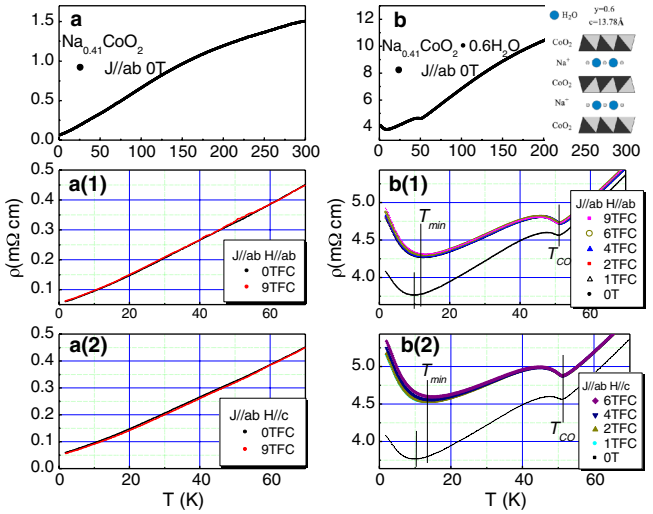

FIG. 2 (color online). ρ_{ab} vs T for $Na_{0.41}CoO_2$ and $Na_{0.41}CoO_2 \bullet 0.6H_2O$. (a) and (b) $\rho(T)$ curves without field, inset of (b) is a structural model of sodium and water arrangement in $Na_{0.41}CoO_2 \bullet 0.6H_2O$. a(1), a(2), and b(1), b(2): ρ vs T curves under various applied fields below 70 K with $H//ab$ and $H//c$.

sentation of the 0.6 water inserted into the structures and the sodium arrangement. The effect of H on ρ_{ab} with $H \parallel c$ is much larger than with $H \parallel ab$ around $T_{\min}$ (see Fig. 2). A large positive magnetoresistance (MR) is observed below 50 K with $H \parallel ab$. The most striking aspect is the second resistivity transition at ~11 K, with a minimum resistivity at $T_{\min}$. $T_{\min}$ increases with H. With increasing H, T_{CO} does not change but $T_{\min}$ does increase. For the case of $H \parallel c$, the MR is much larger than that with $H \parallel ab$ and $T_{\min}$ moves to higher temperature by ~3 K. This indicates a FM characteristic to the 11 K transition.

Turning to the origin of the resistivity below ~11 K, we consider the possibility of the electron-electron scattering with the quadratic temperature dependence of the resistivity: $\rho = \rho_0 + AT^2$. The in-plane $\rho(T)$ of $Na_{0.41}CoO_2 \cdot 0.6H_2O$ at low T is shown in Fig. 3 (upper panel) for different H, plotted as $\rho - \rho_{\text{offset}}$ vs T^2. A T^2 regime is clearly observed for all fields below a crossover temperature T_0 which grows little with field. The observed relation indicates the Fermi-Liquid behavior below near 8 K ($\ll T_{\min}$). However, generic Fermi liquid electron-electron scattering alone cannot explain the resistivity upturn below $T_{\min}$.

We continue by analyzing the dependence of the field dependence of the 11 K transition. As mentioned, there is a large positive MR below 50 K. This is reminiscent of observations in FM $La_{0.7}Ca_{0.3}MnO_3$ films, which show a low T resistivity upturn, originating from quantum interference effects [30]. Using τ_{SO} (spin-orbit scattering time), τ_i (inelastic scattering time), and D (diffusion coefficient), the quantum correction $\delta\sigma_{SO}(T) = \frac{e^2}{2\pi^2\hbar}(3\sqrt{\frac{1}{D\tau_{so}} + \frac{1}{4D\tau_i}} - \sqrt{\frac{1}{4D\tau_i}})$ was taken [31]. D was determined by $\sigma = e^2 N(E_F) D(0)$. A standard $\tau_i \propto T^2$ was assumed [30]. The spin-orbit contribution was obtained by the measured conductivity σ in 9 T subtracted from σ at 0 T. The resulting experimental and theoretical curves are presented in Fig. 3 (lower panel). It is found that the experimental data below 12.7 K can be well fitted with τ_{SO} of 1.38×10^{-11} s and τ_i/T^2 of 5.91×10^{-12} s/K2. Note that this is below $T_{\min}$ in $Na_{0.41}CoO_2 \cdot 0.6H_2O$.

The link between the $T \sim 50$ K CO and $T \sim 11$ K transitions provides a clue to origin of the anomalous in-plane behavior induced by hydration. Both transitions couple to electrons at the FS, as is clear from transport, and also NMR

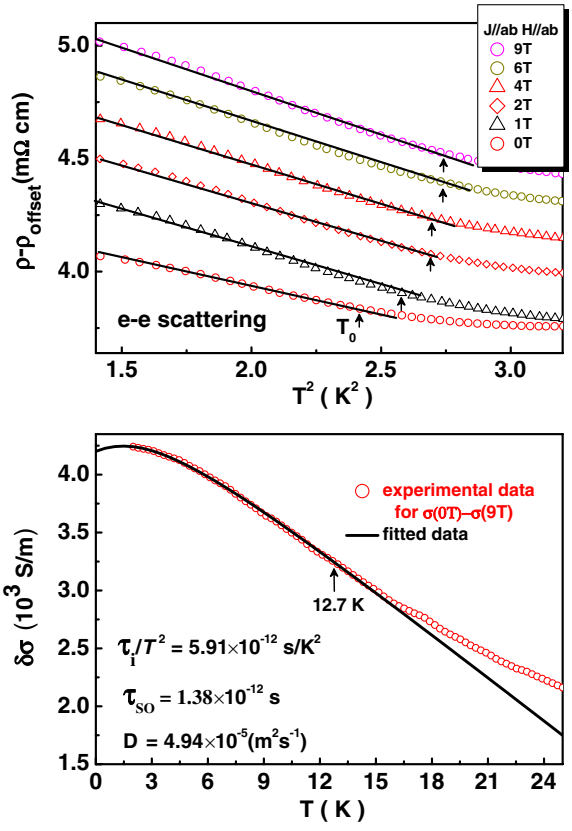

FIG. 3 (color online). Upper panel: $\rho(T) - \rho_{\text{offset}}$ vs T^2 at low temperature for $Na_{0.41}CoO_2 \bullet 0.6H_2O$ at $H = 0$, 1, 2, 4, 6, and 9 T. ρ_{offset} is a constant arbitrary offset chosen for clarity. Lower panel: Zero field spin-orbit coupling.

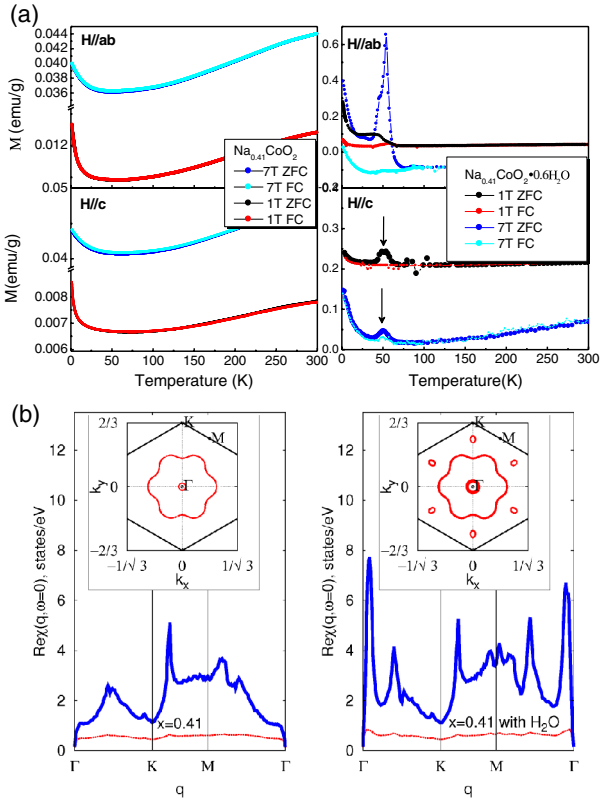

FIG. 4 (color online). (a) $M \sim T$ curves for $Na_{0.41}CoO_2$ and $Na_{0.41}CoO_2 \bullet 0.6H_2O$. (b) Bare ($U = J = 0$, thin red dashed curves) and RPA (thick solid blue curves, $U = 0.7$ eV and $J = 0.35$ eV) physical spin susceptibility Re $\chi(q, \omega = 0)$ vs momentum for $Na_{0.41}CoO_2$ (left) and $Na_{0.41}CoO_2 \bullet 0.6H_2O$ (right). Insets show corresponding FS.

[32]. Figure 4(a) shows that $Na_{0.41}CoO_2 \cdot 0.6H_2O$ develops a more magnetic ground state than the nonhydrated sample. $Na_{0.41}CoO_2 \cdot 0.6H_2O$ shows a Pauli paramagnetic behavior at high temperature, similar to $Na_{0.5}CoO_2$ [11]. The 51 K CO transition is also reflected in the magnetization for $H \parallel ab$ and $H \parallel c$. The low temperature results have an obvious FM tendency, for example, the induced magnetizations are $\sim$10 times higher than in the nonhydrated sample.

Angle-resolved photoemission (ARPES) experiments on fully hydrated $Na_xCoO_2 \cdot yH_2O$ [33] show an extension of the e_g band closer to the Fermi level E_F than in nonhydrated Na_xCoO_2. This suggests perhaps a closer correspondence to band structure results, although the qualitative fact that standard band calculations [19] predict small e_g pockets of FS in addition to the observed a_g large sheet, while these have not been observed in ARPES, remains (note there is evidence for additional FS based on specific heat data [34]). In any case, anomalies have been reported in the hydrated system below 50 K. Besides, the resistivity, discussed above, includes an evolution from a p wavelike to a d wavelike angular-dependent in-plane magnetoresistance (AMR) signal [35]. The concurrence of CO and superconductivity has been discussed in terms of competition of superconducting state and CO state. [14] This is very plausible since superconductivity is a FS instability, and the data discussed above plainly show a very strong interplay of electrons at the FS with charge ordering. Also, there is a very strong connection between magnetism and transport and in fact several studies point to at least partially itinerant magnetic character in these cobaltates as shown by resistivity, magnetoresistance, AMR, and NMR measurements [10,27,36].

To understand the low temperature FM tendency, we calculated the spin susceptibility. As mentioned, there are differences between standard first principles band structures and ARPES experiments. Therefore, we adopt a model based approach following first principles calculations to elucidate the physics in a way that provides information about the effect of different aspects of the electronic structure in a semiquantitative way rather than direct use of the first principles band structure. Since Na_xCoO_2 is a multiorbital system, we use an interaction Hamiltonian, including on-site intra- and interorbital Hubbard repulsions U and U', Hund's coupling J, and the pair hopping $J' = J$ [37].

$$H = H_0 + U\sum_{i,l} n_{il\uparrow}n_{il\downarrow} + J\sum_{i,m}\sum_{\sigma,\sigma'} d^+_{il\sigma}d^+_{im\sigma'}d_{il\sigma}d_{im\sigma} + U'\sum_{i,m<l} n_{il}n_{im} + J'\sum_{i,m\neq l} d^+_{il\uparrow}d^+_{il\downarrow}d_{im\downarrow}d_{im\uparrow}, \quad (1)$$

where $n_{il} = n_{il\uparrow} + n_{il\downarrow}$, $n_{il\sigma} = d^+_{il\sigma}d_{il\sigma}$, $d_{il\sigma}$ is the annihilation operator for the hole on site i, orbital l, with spin σ. For the single-electron Hamiltonian H_0 we use the 3-orbital tight-binding model [38] based on the LDA band structure,

$$H_0 = -\sum_{k,l,\sigma}(\varepsilon^l - \mu)n_{kl\sigma} - \sum_{k,\sigma}\sum_{l,m} t^{lm}_k d^+_{kl\sigma}d_{km\sigma}. \quad (2)$$

where t^{lm}_k is the Fourier transform of the hopping matrix element, ε^l are the single-electron energies, and μ is the chemical potential. Figure 4(b) shows the corresponding FS of nonhydrated $Na_{0.41}CoO_2$ and $Na_{0.41}CoO_2$ with water [39]. It can be seen that the main FS of $Na_{0.41}CoO_2$ is a rounded hexagon. This leads to a number of nesting wave vectors near the AFM wave vector $Q_{\mathrm{AFM}} = \{(\frac{2\pi}{3}, \frac{2\pi}{\sqrt{3}}), (\frac{4\pi}{3}, 0)\}$. With H_2O, the FS has a large a_g pocket around Γ-point of the hexagonal Brillouin zone and six small e_g pockets, which even for very small sizes start to support a FM tendency. This is because of their contribution to the density of states at the Fermi energy, $N(E_F)$. In particular, for a 2D cylinder, $N(E_F)$ is independent of band filling up to the band edge, which is not the case for a 3D pocket. Thus in a highly 2D material like the present hydrated compound, even a very small pocket can contribute to $N(E_F)$ and thus a FM tendency. It should be emphasized that if the band filling is small, the resulting FM moments will also be small and could be suppressed by quantum fluctuations. The same effect would occur if the a_g band adopted a pudding mold shape and an inner Γ-centered FS appeared as a function of doping—a possibility that has been discussed [40].

We study the transverse spin susceptibility $\chi^{ll',mm'}_{+-}(q, \omega)$ in the random phase approximation (RPA) following the multiorbital formalism in Ref. [41] to address the doping dependence. Because of spin-rotational invariance, U' is fixed via $U' = U - 2J$. For $J = 0$ and $x \leq 0.5$ the spin susceptibility shows pronounced peaks at Q_{AFM} reflecting a tendency toward the in-plane 120° AFM order. Increase of J results in the tendency toward the in-plane FM order in the case when e_g FS pockets are present [4]. Figure 4(b) shows real part of the spin susceptibility, $\chi(q, \omega) = \frac{1}{2}\sum_{l,m}\chi^{ll,mm}_{+-}(q, \omega)$, as a function of momentum at $\omega = 0$. Interaction parameters are chosen to stay right below the magnetic instability; a slight increase of U and/or J results in ordering. Thus the position of the peak indicates the ordering wave vector in the magnetic phase. For $Na_{0.41}CoO_2$ with water, the largest peak is near $k = 0$ indicating a tendency toward FM. This further supports the FM tendency of the 11 K transition. The origin of this is due to the large $N(E_F)$ and the relatively large $J \sim U/2$. The bottom line is that there are two reasons that can be proposed for in-plane FM at low temperatures. Both explanations involve an assumption that the intercalated water not only acts as a spacer, but also either provides additional doping or changes the band structure to simulate the effect of doping on the nesting. The first is that in $Na_{0.41}CoO_2 \cdot 0.6H_2O$ the e_g pockets are present. The fact that e_g bands are pushed toward the Fermi level upon water intercalation was confirmed by ARPES [7], while they are

[32] F. L. Ning, T. Imai, B. W. Statt, and F. C. Chou, Phys. Rev. Lett. **93**, 237201 (2004).
[33] T. Shimojima, K. Ishizaka, S. Tsuda, T. Kiss, T. Yokoya, A. Chainani, S. Shin, P. Badica, K. Yamada, and K. Togano, Phys. Rev. Lett. **97**, 267003 (2006).
[34] N. Oeschler, R. A. Fisher, N. E. Phillips, J. E. Gordon, M. L. Foo, and R. J. Cava, Phys. Rev. B **78**, 054528 (2008).
[35] C. H. Wang, X. H. Chen, G. Wu, T. Wu, H. T. Zhang, J. L. Luo, G. T. Liu, and N. L. Wang, Phys. Rev. B **74**, 172507 (2006).
[36] J. L. Gavilano, B. Pedrini, K. Magishi, J. Hinderer, M. Weller, H. R. Ott, S. M. Kazakov, and J. Karpinski, Phys. Rev. B **74**, 064410 (2006).
[37] C. Castellani, C. R. Natoli, and J. Ranninger, Phys. Rev. B **18**, 4945 (1978).
[38] M. M. Korshunov, I. Eremin, A. Shorikov, V. I. Anisimov, M. Renner, and W. Brenig, Phys. Rev. B **75**, 094511 (2007).
[39] For the FS calculation of hydrated $Na_{0.41}CoO_2$, we decrease the a_g-e_g crystal field splitting and thereby push the e_g band to the Fermi level. The splitting was decreased by 10 meV.
[40] D. Yoshizumi, Y. Muraoka, Y. Okamoto, Y. Kiuchi, J. I. Yamaura, M. Mochizuki, M. Ogata, and Z. Hiroi, J. Phys. Soc. Jpn. **76**, 063705 (2007).
[41] S. Graser, T. A. Maier, P. J. Hirschfeld, and D. J. Scalapino, New J. Phys. **11**, 025016 (2009).
[42] N. B. Ivanova, S. G. Ovchinnikov, M. M. Korshunov, I. M. Eremin, and N. V. Kazak, Phys. Usp. **52**, 789 (2009).